Proton-Decoupled ^{31}P Chemical Shift Imaging of the Human Brain in Normal Volunteers

Joseph Murphy-Boesch,* Radka Stoyanova,† Ravi Srinivasan,† Tamela Willard,† Daniel Vigneron,‡ Sarah Nelson,‡ June S. Taylor§ and Truman R. Brown†

†Department of NMR, Fox Chase Cancer Center, 7701 Burholme Avenue, Philadelphia, PA 19111, ‡Department of Radiology, University of California, San Francisco, CA 94143-0288 and §Department of Diagnostic Imaging, 332 N. Lauderdale, Memphis, TN 38101-0318, USA

Proton-decoupled, ^{31}P three-dimensional (3-D) chemical shift imaging (CSI) spectra have been acquired from the entire human brain using a new dual tuned resonator. The resonator operates in quadrature mode to provide improved sensitivity, excellent B_1 homogeneity, and reduced power deposition at both frequencies. Proton-decoupled and fully NOE enhanced, ^{31}P spectra were acquired from normal volunteers using Waltz-4 proton decoupling with continuous wave bi-level excitation applied through a second radio frequency channel. Well resolved peaks in the phosphomonoester (PME) and phosphodiester regions were obtained from non-localized FIDs and spectra localized with 3-D CSI without processing for resolution enhancement. pH measurements made over large regions of the brain using the P_i resonance show no significant variations (6.9±0.02) for a single individual. The improved spectral resolution and sensitivity of the PME resonances results in more well defined metabolite images of the PME peak region.

INTRODUCTION

It has been known for many years that proton decoupling will collapse the doublet, triplet, and higher order multiplet structures imposed upon the spectra of ^{31}P and other low-γ nuclei by neighboring ^{1}H nuclei. These J-couplings are typically 5–10 Hz which are greater than the spectral linewidths which now can be achieved for localized ^{31}P spectra at 1.5 T. Recognizing this, Luyten *et al.*[1] have used proton decoupling in conjunction with a single voxel localization technique (ISIS) to obtain well resolved ^{31}P spectra from human muscle, liver, brain and heart. Because of low spectral resolution in the coupled case, the resonances in the phosphomonoester (PME) and phosphodiester (PDE) regions generally produce broad peaks which cannot be assigned to specific compounds. Using proton decoupling during acquisition and resolution enhancement of the processed spectra, they were able to observe well-resolved resonances of phosphocholine (PC), phosphoethanolamine (PE), glycerophosphocholine (GPC) and glycerophosphoethanolamine (GPE) from a 200 cm^3 voxel in the brain. In addition to improvements in spectral resolution from decoupling, phosphorus sensitivity may also be enhanced during proton irradiation via the nuclear Overhauser effect (NOE), which, in the case of dipolar coupling, can increase the ^{31}P signal by one-half the ratio of their gyromagnetic ratios, or 1.24.[2] Partial NOE enhancement occurs when using proton decoupling, because of partial saturation of the proton resonances. Luyten *et al.*, however, evidently observed little NOE enhancement, owing to their long recycle time (3.0–3.5 s). Partial NOE enhancement of phosphorus metabolite resonances from a single 125 cm^3 voxel in the brain has been observed by Merboldt and co-workers using a STEAM sequence,[3] with similar results having been observed in muscle,[4] although in neither case was any proton irradiation applied outside of the data acquisition period.

We have developed localized, proton-decoupled ^{31}P spectroscopy of the human brain which differs from previous studies in several respects. We use chemical shift imaging (CSI) techniques[5–13] to obtain spectra from smaller localized voxels. The three-dimensional (3-D) CSI technique uses a simple pulse sequence (an excitation pulse, followed by short phase encoding gradient pulses in three dimensions) to obtain a 3-D array of multiple spectra from contiguous voxels throughout the subject under study. The spectral information of these voxels can then be converted into images of individual metabolites.[11,14] To the CSI sequence we have added proton decoupling during the acquisition period using Waltz-4 modulation.[15] Additionally, we use low-level continuous wave (CW) excitation between acquisition periods for full NOE enhancement. This 'bi-level' proton excitation provides both improved spectral definition with decoupling and improved sensitivity from collapse of multiplets to single resonances and NOE enhancement. Finally, we obtain additional sensitivity from the brain using a new quadrature dual tuned head coil, which has been developed in our laboratory.[16–18] Operating in quadrature mode at both the ^{1}H and ^{31}P frequencies, this resonator provides both improved sensitivity during reception and lower power deposition for broadband decoupling. The resonator has also been used to shim the static field and acquire high-quality ^{1}H images, greatly facilitating our examination protocols. Here, we present coupled and proton-decoupled spectra from CSI examinations of two volunteers at 43 and 18 cm^3 voxel size to provide

* Author to whom correspondence should be addressed.

Abbreviations used: PME, phosphomonoester; PDE, phosphodiester; PC, phosphocholine; PE, phosphoethanolamine; GPC, glycerophosphocholine; GPE, glycerophosphoethanolamine; NOE, nuclear Overhauser effect; CSI, chemical shift imaging; 3-D, three-dimensional; CW, continuous wave; SAR, specific absorption rates; PCr, phosphocreatine.

0952–3480/93/030173–08 $09.00

Received 3 March 1992
Accepted (revised) 11 December 1992

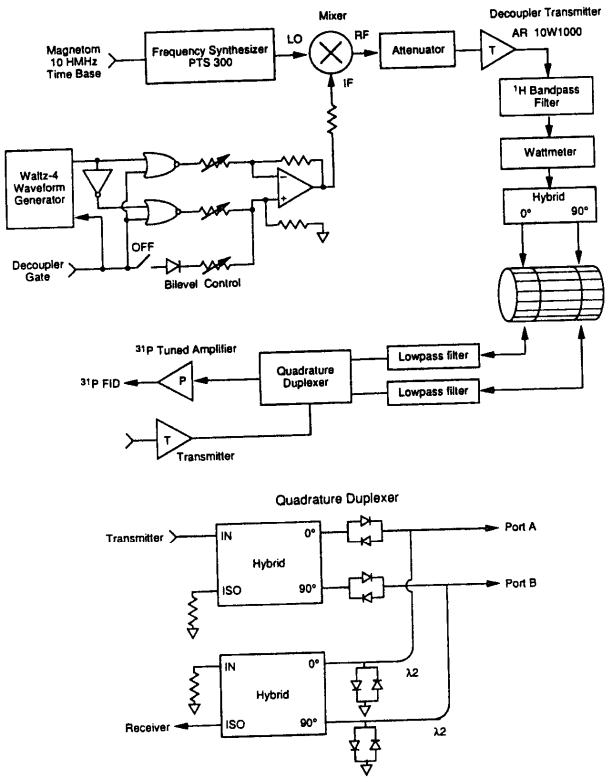

Figure 1. Second radio frequency channel integrated into the Siemens Magnetom transmitter/receiver electronics for acquisition of proton-decoupled ^{31}P spectra.

voxel-by-voxel comparisons and also to demonstrate the spectral improvements from decoupling and NOE and the improved sensitivity of the quadrature coil.

METHODS

All CSI examinations were performed with a 1.5 T Siemens Magnetom clinical imager/spectrometer (Siemens AG, Erlangen, Germany). To this was added a second RF channel, shown in Fig. 1. This RF channel was developed and configured to provide the constant amplitude phase modulated proton-decoupling power during the acquisition of phosphorus signals and also the low power CW or bi-level excitation between acquisitions for NOE enhancement. Broadband decoupling was implemented using Waltz-4 modulation[15] gated with a sequence programmable signal from the spectrometer. Between acquisitions, low-level CW power was gated by delivering a constant offset current to the mixer. Decoupler power was derived from a 10 W transmitter (Amplifier Research, Souderton, PA), which was limited by driving the transmitter into saturation during decoupling. The transmitter's output was bandpass filtered at the proton frequency to eliminate harmonics and noise at the phosphorus frequency, monitored with a Bird Model 442 watt meter (Bird Electronic Corp., Cleveland, OH), and fused near the coil to limit power. When acquiring proton-decoupled ^{31}P FIDs and CSI data sets, 13 W of decoupling power were delivered during acquisition (0.256 s) and 1.5 W CW power between acquisitions (0.744 s). Total average power delivered to the coil was 4.4 W, yielding specific absorption rates (SAR) of 1.0–1.5 W/kg, assuming all power was absorbed by the head. This provided a nominal decoupling bandwidth of ±200 Hz (1.25 ms 90° clock cycle) for the Waltz-4 sequence.

Images and spectra were acquired using a custom-built, dual tuned birdcage resonator,[16–18] which operates in quadrature (circularly polarized) mode simultaneously at both ^{31}P and ^{1}H frequencies (25.7 and 65.7 MHz, respectively). The coil is a four-ring birdcage design with both the inner and outer structures in the low-pass configuration. The coil has 16 legs, an inner ring spacing of 12.5 cm, an overall length (outer ring spacing) of 25 cm, and a diameter of 26.7 cm. From computed field plots, the B_1 field distribution at the phosphorus frequency is similar to that of a 12.5 cm long conventional two-ring birdcage.[8,18] The B_1 field distribution at the proton frequency is homogeneous over the brain to within ±10%, providing uniform decoupling of the proton resonances.[18] As indicated in Fig. 1, each of the quadrature duplexers for the coil employs two quadrature hybrids (Triangle Microwave, East Hanover, NJ) and duplicate quarter-wavelength, crossed-diode networks[19] for transmit/receive switching. Two such duplexers were constructed, one for each of the NMR frequencies. Custom built low-pass filters with matched characteristics were installed between the coil and phosphorus receiver circuitry to reduce the level of the decoupling signals passing through the coil and entering the receiver circuitry. Phosphorus signals were combined in the receiver hybrid and passed to a Siemens preamplifier tuned to the ^{31}P frequency (NF = 1.3 dB). For acquisition of ^{31}P data, two four-pole Butterworth audio filters with matched gain and matched bandwidths of 1 kHz were constructed and used in place of the Siemens filters for optimum detection bandwidth and rapid recovery.

At the beginning of an examination, the subject was positioned, and the coil tuned and isolated (mode aligned) at both the phosphorus and proton frequencies. Scout ^{1}H images were acquired for positioning. Then, a series of T_1-weighted (400/17) proton images were acquired for anatomical referencing and metabolite image overlays, with nine images acquired in each of the three orientations. The ^{1}H water signal from the head was used to shim the static B_0 field to 20–25 Hz (linewidth at half-height). Upon switching to the phosphorus frequency the frequency of the decoupler was set to 1.0 ppm below the water resonance, in the region of the proton spectrum occupied by protons coupled to the phosphates of the PMEs and PDEs. Non-localized FIDs were acquired, both coupled and decoupled, using a rectangular 250 μs pulse, 512 points, 64 acquisitions and a TR of 1 s. The voltage of the pulse was adjusted to provide a tip angle of 40° at the center of the coil (the Ernst angle for $T_1 = 4$ s). 3-D CSI data sets were then acquired using the same 250 μs RF pulse followed by triangular 2.1 ms phase encode gradients applied in each of the three orientations and acquisition of 512 data points (256 ms). CSI data sets were acquired in $8 \times 8 \times 8$ arrays with six acquisitions per phase encode step and a $TR = 1$ s for a total acquisition time of 51 min. Data were transferred off-line for archiving, processing and display. All examinations were performed under institutional review board approval.

All data, including images and spectra, were processed on a VAX 8800 (Digital Equipment, Inc.,

Maynard, MA) using software developed in this laboratory.[11,20,21] To process the four-dimensional CSI data sets, raw data were first Fourier transformed in the three spatial dimensions. Five initial time points of each FID were then zeroed and a (1–5 Hz) Lorentzian filter applied before final Fourier transformation of the time dimension. The phasing parameters for the spectrum of the non-localized FID were used to phase all spectra in the CSI array. The rolling baseline caused by the absence of the five initial time points was removed by first fitting a baseline to each CSI spectrum using a linear-quadratic estimator[21] outside the peak regions identified in the non-localized spectrum and then subtracting the baseline estimate from the spectrum. Smaller arrays of spectra were extracted and displayed on the same scale for voxel-by-voxel comparison of coupled and decoupled data. Chemical shifts of P_i were measured relative to the phosphocreatine (PCr) peak position, which was set to -2.52 ppm (phosphoric acid = 0.0 ppm), and were converted to pH using a Henderson–Hesselbach equation with the parameters $pK_a = 6.718$, $\delta_{acid} = 0.591$ and $\delta_{alkaline} = 3.187$.

Metabolite images were constructed for single ^{31}P resonances using peak area estimates from each spectrum in a $16 \times 16 \times 16$ array (the original $8 \times 8 \times 8$ zero-filled once in each spatial dimension). A modified PIQABLE algorithm[20,21] was used for automatic baseline estimation (linear-quadratic) and estimation of the peak areas for all spectra. Initial estimates of the peak regions were made from the non-localized FID. The algorithm then estimated the baseline and refined the peak regions for the spectrum of each voxel. Using these baseline estimates and peak regions, the algorithm then returned the maximum integral in the peak region as an estimate for the peak area of each metabolite. An image was then created by interpolating the $16 \times 16 \times 16$ array of area estimates to $32 \times 32 \times 32$ and the output displayed in three orientations as multi-slice metabolite images or as color overlays upon the proton image for direct correlation with anatomy. For display of metabolite images, negative signals (due to noise) were set to zero.

RESULTS

To demonstrate improvements in the quality of ^{31}P spectra from proton irradiation, coupled and proton-decoupled data were acquired consecutively within single examinations of several volunteers to provide both non-localized and voxel-by-voxel comparisons. Consecutive CSI data sets were acquired from one volunteer at 43 cm^3 (3.5 cm × 3.5 cm × 3.5 cm) resolution, and the non-localized FIDs for this individual, coupled and decoupled, are shown in Fig. 2. The greatest improvements in resolution are in the PDE and α-NTP peak regions where individual resonances can now be observed. In addition, the sensitivity of the PME region is clearly enhanced and the region is better resolved. The PCr peak shows a ca 30% increase in signal intensity. In Fig. 2(c) the decoupled spectrum was further processed using convolution difference to remove the broad component in the baseline, and Gaussian and exponential multiplication in the time-domain for resolution. The processing parameters used (see figure legend) were chosen so that we could compare our results with those of Luyten *et al.*[1] The agreement is excellent, particularly in view of the fact that we are comparing a spectrum from the whole head with one localized to 200 cm^3 in the left cerebral hemisphere.

Similar results can be observed in a comparison of spectra from the individual CSI voxels. Coupled and decoupled spectra from four voxels along the midline of the brain, as indicated in the images of Fig. 3, are presented on the same scale in Fig. 4. As in the non-localized case, well resolved resonances appear in the proton decoupled PME, PDE, and α-NTP peak regions making it possible to assign these resonances to individual metabolites. No resolution enhancement has been used so that the peak areas of these resonances are quantifiable. In addition to the improved spectral resolution, there is an increase in signal intensity from NOE enhancement for some of the resonances. In the four spectra shown in Fig. 4, the PCr peak increased in intensity by 30±10% (means±SD) upon proton irradiation, but no significant line narrowing was observed. Little or no NOE enhancement was observed for any of the NTP peaks. The broad linewidths of the PME and PDE peaks and their low sensitivity in the coupled case makes comparisons of areas from a single voxel unreliable for NOE measurement. Further, the oscillating baseline originating from the five zeroed early time points introduced significant errors in the estimated peak areas of broad resonances. To provide better NOE estimates, spectra from all the voxels in the same axial slice were added together to increase sensitivity.

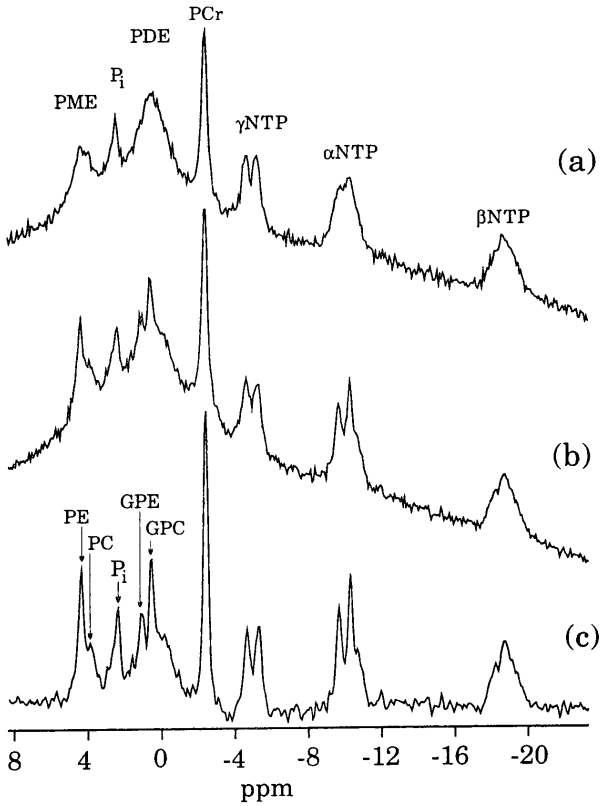

Figure 2. Non-localized ^{31}P spectra from the entire head displayed with the same vertical scale: (a) coupled and (b) proton-decoupled, processed with no line broadening, and (c) the proton-decoupled data of (b) processed using 200 Hz Gaussian deconvolution (0.8 subtraction factor) followed by 6 Hz Gaussian and −5 Hz exponential filters.

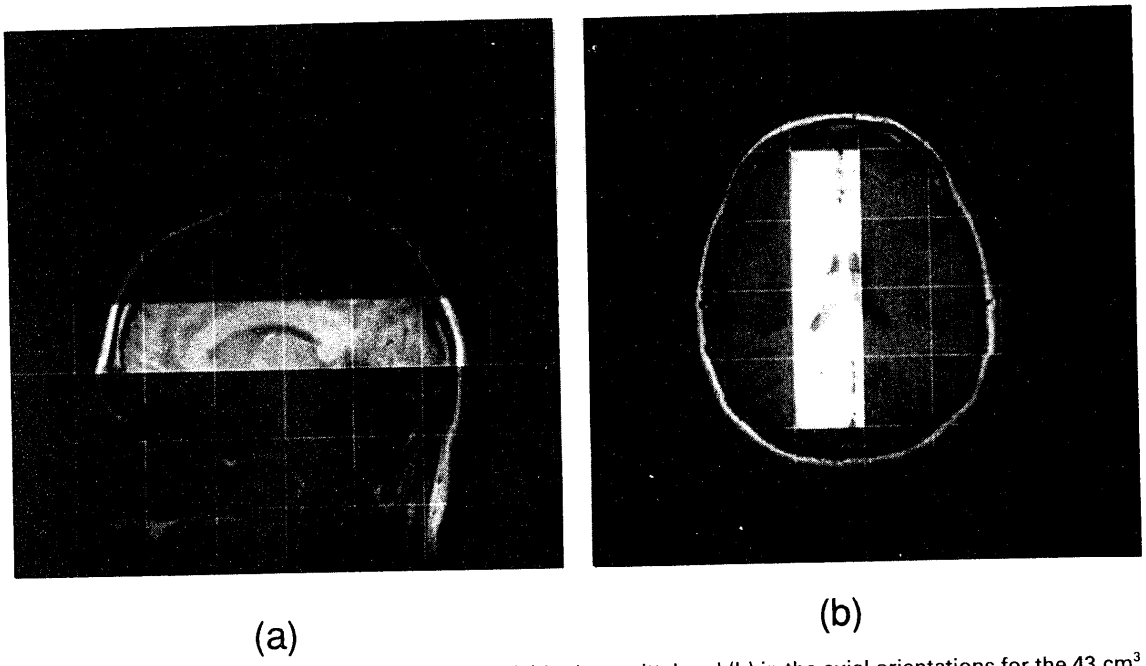

Figure 3. T_1 weighted proton images of the brain (a) in the sagittal and (b) in the axial orientations for the 43 cm^3 (3.5 cm × 3.5 cm × 3.5 cm) examination. The grid indicates the position of the CSI array after voxel shifting of CSI spectra; highlighting indicates the slice and position of the voxels from which the spectra in Fig. 4 were taken.

The areas of various peaks were then determined in the irradiated and non-irradiated cases to estimate the NOE enhancements for this individual, which were ca 60, 25 and 25% for PME, P_i and PCr, respectively. The peak areas of the NTP resonances were the same to within 10%. Even with the addition of the spectra, it was still not possible to evaluate the NOE enhancement in the PDE region because of the presence of a broad peak believed to originate from partially motionally narrowed resonances of phospholipids[22] in the coupled spectrum. The static field homogeneity in the brain could be followed by monitoring the linewidth of the PCr peak. In Fig. 4(b), the third voxel is better shimmed than the others, possibly due to the absence of nearby air–tissue interfaces. The natural linewidth of PCr for this voxel was ca 3 Hz. The PME region of this spectrum shows peaks at the chemical shifts expected for PE and PC (4.32 and 3.79 ppm, respectively). Although this does not constitute absolute proof that these peaks correspond to these compounds, they are well known to exist in the brain[23] and are by far the most likely assignments for these two resonances. The PDE region similarly shows two peaks resolved with chemical shifts appropriate for GPC and GPE (0.49 and 1.03 ppm, respectively).

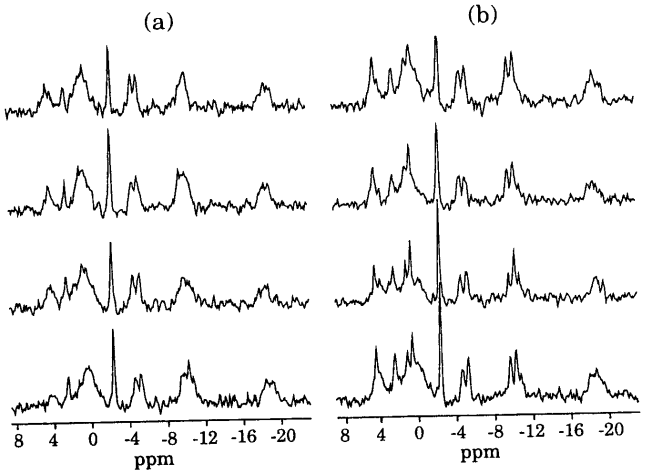

Figure 4. (a) Coupled and (b) decoupled CSI spectra at 43 cm^3 voxel size from the voxels highlighted in Fig. 3 displayed on the same scale. Both CSI data sets were acquired consecutively from the same volunteer with identical acquisition parameters, except for proton irradiation. Filtering in the time-domain for both sets consisted only of a 3 Hz Lorenzian. Baselines estimated for each spectrum have been subtracted.

At higher spatial resolutions the increased resolution and sensitivity from proton irradiation can be used to improve the quality of the metabolic images constructed from the data. To demonstrate this, coupled and decoupled CSI spectra were acquired at 18 cm^3 (2.6 cm × 2.6 cm × 2.6 cm) voxel resolution in consecutive 51 min examinations from a second volunteer. Coupled and decoupled spectra from an axial slice at approximately the same elevation in the brain as the first volunteer are shown in Figs 5(a) and (b), respectively. Metabolite images of the entire PME peak region were constructed from both data sets without spatial filtering or correction for the field profile of the coil and are shown on the same scale in Fig. 6. As one can see, the axial profile of the head is far better defined in the decoupled case than the coupled case, owing to both the improved resolution and signal intensity of the PME metabolites. Some increased signal intensity results from the increased B_1 field around the periphery of the head. Some variations in intensity of the images in the region of the head are related to errors in baseline estimates, and some decrease in intensity of phosphates in the mid-brain region results from the presence of the ventricles. In both the coupled and decoupled data sets, the chemical shift of P_i could be determined more reliably in better shimmed voxels. In the presence of proton irradiation, however, more determinations could be made at this voxel resolution with the improved resolution of the PME and PDE resonances on either side of the P_i resonance. In the present circumstances, no significant variations were

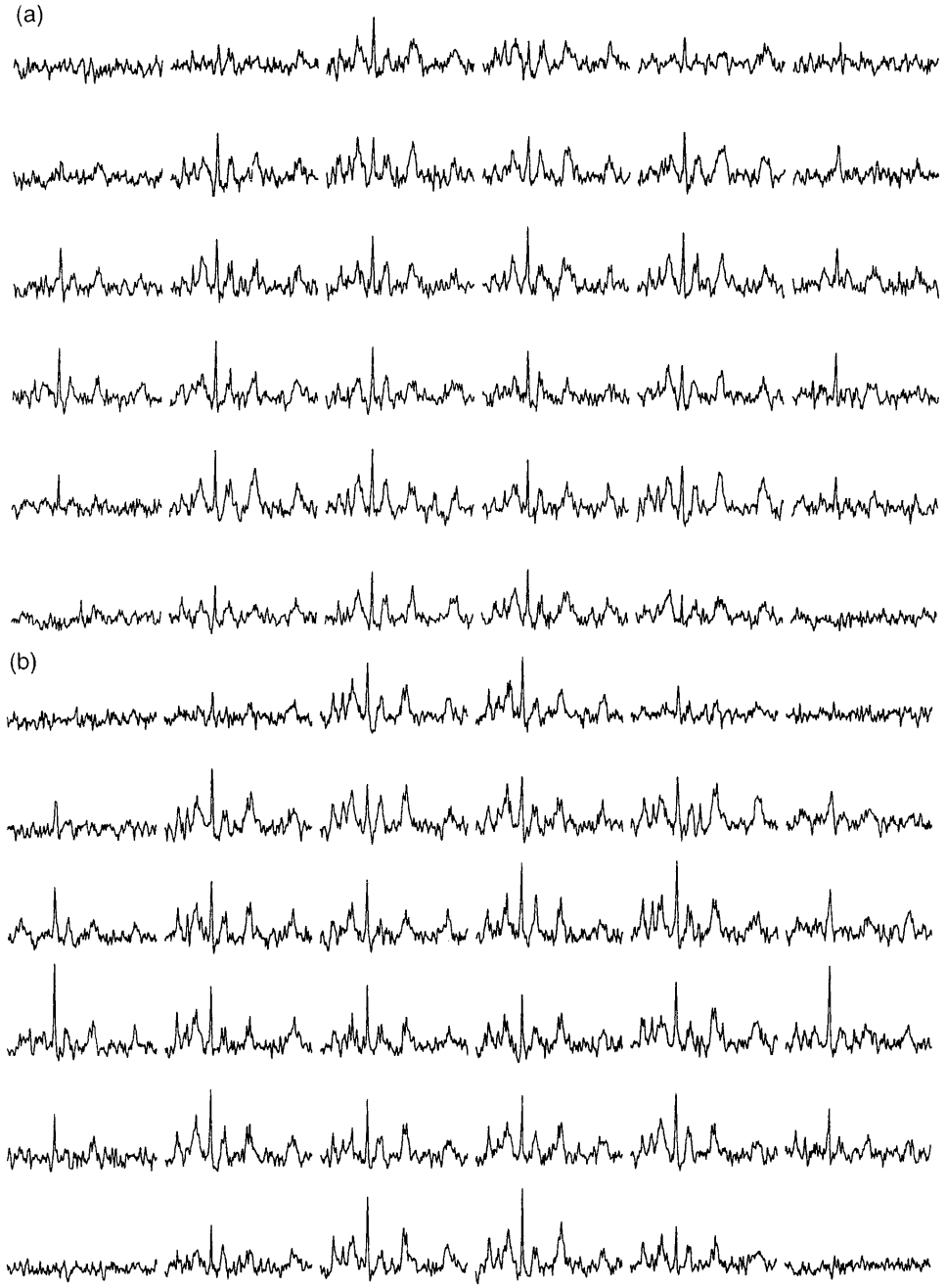

Figure 5. (a) Coupled and (b) decoupled CSI spectra acquired consecutively from a second volunteer at 18 cm^3 (2.6 cm × 2.6 cm × 2.6 cm) resolution. Spectra were taken from an axial slice at approximately the same elevation in the brain as the 43 cm^3 data set (see Fig. 3). The FIDs were zero filled to 1024 points and filtered with a 5 Hz Lorenzian. Baselines estimated for each spectrum have been subtracted, and only the center 6 × 6 array of spectra of a single 8 × 8 slice are shown.

seen in the P_i peak position for this individual; its mean position and SD were 2.28±0.05 ppm, which corresponds to a pH of 6.9±0.02.

DISCUSSION

Acquisition of decoupled spectra in these studies was facilitated with the use of the dual tuned head coil operating in circularly polarized mode at both the phosphorous and proton frequencies. The acquisition of proton images as well as the decoupling permitted by this resonator greatly simplifies the overall examination by allowing integrated $^{1}H/^{31}P$ observations without mid-examination movement of the subject. The sensitivity of this coil is 100±5% at the phosphorus frequency and 85±5% at the proton frequency compared with equivalent single tuned coils, and power deposition in the head at the proton frequency is approximately a factor of two lower than a coil operating in linear mode; e.g., a crossed Helmholtz design. This has made it possible to remain well within the FDA guidelines for power deposition while obtaining both full decoupling and NOE. The high ^{31}P sensitivity meant that we achieved virtually all of the increased sensitivity possible from the proton irradiation.

The effects of proton irradiation on the ^{31}P spectra, both localized and non-localized, are two-fold: the improved spectral resolution due to the collapse of the

^{1}H-^{31}P multiplet structures and an increase in peak amplitude from NOE enhancement. These two effects arise from quite different interactions and thus are induced by different proton power levels. To achieve decoupling, the power level must be sufficient to average out a J coupling of 10 Hz. This means proton B_1 fields should be strong enough to average out a proton's spin state in <100 ms. The NOE enhancement on the other hand can be achieved by only saturating the proton spins. This requires substantially less power since the typical T_1 is 500 ms. Thus, bi-level power was used: 13 W during acquisition to achieve decoupling and 1.5 W during recovery to maintain proton saturation. Assuming water protons are the dominant relaxation pathway for ^{31}P in tissue,[24] we can estimate the effects of our CW radiation 1 ppm downfield from water.[2] Taking a $T_1 = 500$ ms and a $T_2 = 50$ ms, the water protons are >90% saturated by this radiation. The same computation would yield a saturation of 99% using the magnitude of the decoupling field (200 Hz), although the saturation effect of this irradiation is complicated by the Waltz-4 modulation. Nevertheless, we should thus be observing at least 90% of any possible NOE from water protons. Bi-level irradiation with CW was chosen over other ^{1}H excitation, such non-selective 180° pulses,[25] because of its ease of implementation, the relatively small power it contributes (25% of total), and its independence of the *TR* and the T_1s of the individual metabolites. Although we have not yet studied enough individuals to report population values for the NOE enhancements in brain, the observed differences in NOE enhancements between the individuals we have studied appear to be small. Interestingly, while NTP exhibits almost no NOE enhancement in brain, a significant NOE enhancement is observed in calf muscle.[3,26,27] This tissue difference means that a localized study is needed to determine the NOE enhancements in the brain, since any measurements on the whole head would be contaminated by muscle.

Decoupling of the ^{1}H-^{31}P multiplet structure is particularly useful in the PME and PDE regions. As can be seen from the spectra shown in Figs 2, 4 and 6, substantial improvements in resolution, and thus, metabolite identification, are apparent. The PDE region shows two narrow peaks which correspond in chemical shift to GPE and GPC. These peaks overlap a much broader peak which presumably arises from the head groups of the phospholipids in the cell membranes.[22] The PME region similarly shows two peaks which have chemical shifts appropriate for PE and PC at pH 7. PE and PC are known to exist in brain (PE at a concentration of 1.1 mM),[23] thought to be altered in tumors,[28–30] and may be involved in some of the fundamental processes involving cell division.[31] The ability to distinguish and measure the amounts of these compounds present in brain tumors may provide a unique window to the biochemistry of this important class of brain pathologies. Since animal experiments suggest the relative amounts of PC or PE can be a measure of therapeutic response,[29] the ability to measure the two compounds individually is potentially of great importance. Although our processing software does not now separate the individual resonances of these compounds, future developments which will apply techniques to resolve multicomponent lines to the individual spectra from each voxel will permit us to determine the spatial distributions of each of these compounds individually.

In addition to the increase in resolution in the PME and PDE regions, the reduction of overlap with the P_i peak improves our ability to observe P_i in voxels throughout the brain. Resolving P_i accurately makes it possible to determine both its spatial distribution and, from its chemical shift, the regional pH, a parameter of considerable importance for many brain dysfunctions. It is likely that the P_i concentration is also a parameter of considerable importance since it is so closely coupled to the amount of available metabolic energy through the NTP free energy. In animal model studies, strong

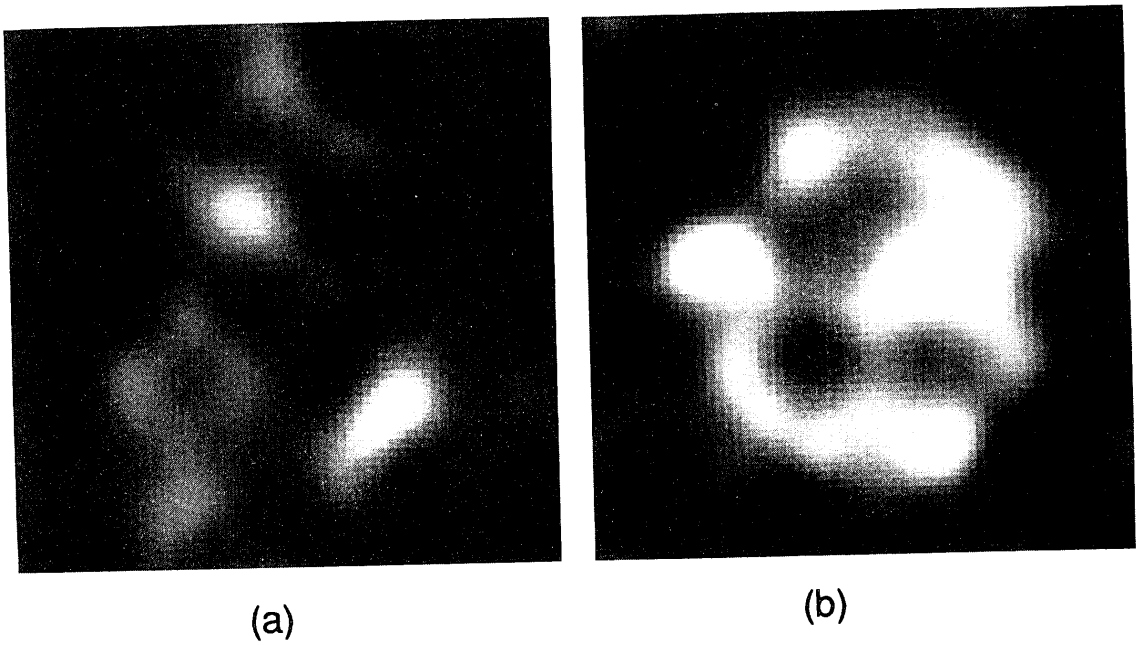

Figure 6. Metabolite images of PME constructed from (a) coupled and (b) the decoupled CSI datasets of Figs 5(a) and (b), respectively. Intensities are scaled to the maximum intensity of the decoupled data.

correlations have been observed between the P_i/NTP ratio and various measures of brain function.[32] Thus, it is reasonable to expect that P_i will be a sensitive measure of regional brain metabolism.

In summary, the improved sensitivity and resolution from bi-level decoupling has made it possible to identify individual resonances in previously featureless regions. Although we previously have been able to obtain PME images from coupled spectra, the decoupled data clearly improves their sensitivity, as the images in Fig. 6 illustrate. In addition, we are now able to observe more clearly the P_i peak. These results demonstrate that the addition of proton bi-level decoupling to ^{31}P CSI examinations, particularly in the brain, produces a substantial improvement in data quality and interpretation which more than compensates for the added technical complexity.

Acknowledgements

The authors gratefully acknowledge the technical support provided by Edward Kosinski and Titia Heddema-Scherpbier for data processing, Chris Elsasser, John Moeller and Lucas Carvajal for mechanical and electronic development, and Jo Anne Bowman, Jeanette Hengy, Jean Fink and Donna Morrissey for administrative support and manuscript preparation. We thank also Drs Benjamin Szwergold, Frank Kappler, Robert Graham and William Negendank for many helpful discussions and preparation of samples, and James Hildenberger of Siemens Medical Systems for technical help with the clinical instrument. This work was supported by NIH grants CA49516, CA41078, CA06927, and NSF grant DIR8904066, and Siemens Medical Systems.

REFERENCES

1. Luyten, P. R., Bruntink, G., Sloff, F. M., Vermeulen, W. A. H., van der Heijden, J. I., den Hollander, J. A. and Heerschap, A. Broadband proton decoupling in human ^{31}P. *NMR Biomed.* **1**, 177–183 (1989).
2. Noggle, J. H. and Shirmer, R. E. *The Nuclear Overhauser Effect.* Academic Press, San Diego (1971).
3. Merboldt, K. D., Chien, D., Hanicke, W., Gyngell, M. S., Bruhn, H. and Frahm, J. Localized ^{31}P NMR spectroscopy of the adult human brain *in vivo* using stimulated-echo (STEAM) sequences. *J. Magn. Reson.* **89**, 343–361 (1990).
4. Bachert-Baumann, P., Ermark, F., Zabel, H.-J., Sauter, R., Semmler, W. and Lorenz, W. J. *In vivo* nuclear Overhauser effect in ^{31}P-{^{1}H} double resonance experiments in a 1.5 T whole-body MR system. *Magn. Reson. Med.* **15**, 165–172 (1990).
5. Brown, T. R., Kincaid, B. M. and Ugurbil, K. NMR chemical shift imaging in three dimensions. *Proc. Natl. Acad. Sci. USA* **79**, 523–526 (1982).
6. Maudsley, A. A., Hilal, S. K., Perman, W. H. and Simon, H. E. Spatially resolved high resolution spectroscopy by four-dimensional NMR. *J. Magn. Reson.* **51**, 147–152 (1983).
7. Brown, T. R., Buchthal, S., Murphy-Boesch, J., Nelson, S. J. and Taylor, J. T. A multi-slice sequence for ^{31}P *in vivo* spectroscopy: 1-D chemical shift imaging with an adiabatic-half passage pulse. *J. Magn. Reson.* **82**, 629–633 (1989).
8. Bottomley, P. A., Charles, H. C., Roemer, P. B., Flamig, D., Engeseth, H., Edelstein, W. A. and Mueller, O. M. Human *in vivo* phosphate metabolite imaging with ^{31}P NMR. *Magn. Reson. Med.* **7**, 319–336 (1988).
9. Coutts, G. A., Bryant, D. J., Collins, A. G., Cox, I. J., Sargentoni, J. and Gadian, D. G. ^{31}P magnetic resonance spectroscopy of the normal human brain: approaches using four-dimensional chemical shift imaging and phase mapping techniques. *NMR Biomed.* **1**, 190–197 (1989).
10. Ross, D. R., Tropp, J., Derby, K. A., Sugiura, S., Hawryszko, C., Jacques, D. B. and Ingram, M. Metabolic response of glioblastoma to adoptive immunotherapy: detection by phosphorus MR spectroscopy. *J. Compt. Ass. Tomography* **13**, 189–193 (1989).
11. Vigneron, D. B., Nelson, S. J., Murphy-Boesch, J., Kelley, D. A. C., Kessler, H. B., Brown, T. R. and Taylor, J. S. Chemical shift imaging of human brain: axial, sagittal, and coronal P-31 metabolite images. *Radiology* **177**, 643–649 (1990).
12. Vigneron, D. B., Taylor, J. S., Nelson, S. J., Murphy-Boesch, J., Kessler, H. B., Curran, W., Coia, L. and Brown, T. R. Studies of metastatic brain tumors using three dimensional ^{31}P metabolite imaging. *9th Annual Meeting of the Society of Magnetic Resonance in Medicine.* Abstr., p. 141 (1990).
13. Maudsley, A. A., Twieg, D. B., Sappey-Marinier, D., Hubesch, B., Hugg, J. W., Matson, G. B. and Weiner, M. W. Spin echo ^{31}P spectroscopic imaging in the human brain. *Magn. Reson. Med.* **14**, 415–422 (1990).
14. Nelson, S. J., Taylor, J. S., Vigneron, D. B., Murphy-Boesch, J. and Brown, T. R. Imaging of ^{31}P metabolites in the human arm. *NMR Biomed.* **4**, 268–273 (1991).
15. Shaka, A. J., Keeler, J. and Freeman, R. Evaluation of a new broadband decoupling sequence: Waltz-16. *J. Magn. Reson.* **53**, 313–340 (1983).
16. Murphy-Boesch, J., Srinivasan, R. and Brown, T. R. P-31/H-1 Dual-tuned quadrature birdcage head coil for clinical imaging and proton-decoupled spectroscopy at 1.5 T. *Radiology* **177**, 309 (1990).
17. Murphy-Boesch, J., Srinivasan, R. and Brown, T. R. A dual tuned four-ring birdcage resonator for ^{1}H decoupled ^{31}P spectroscopy of the human head at 1.5 Tesla. *10th Annual Meeting of the Society of Magnetic Resonance in Medicine.* Abstr., p. 717 (1991).
18. Murphy-Boesch, J., Srinivasan, R., Carvajal, L. and Brown, T. R. Two configurations of the four-ring birdcage for ^{1}H imaging and ^{1}H-decoupled ^{31}P spectroscopy of the human head. *J. Magn. Reson.* (in press).
19. Lowe, I. J. and Tarr, C. E. A fast recovery probe and receiver for pulsed nuclear magnetic resonance spectroscopy. *J. Sci. Instrum.* **1**, 320–322 (1968).
20. Nelson, S. J. and Brown, T. R. A method for automatic quantification of one-dimensional spectra with low signal-to-noise ratio. *J. Magn. Reson.* **75**, 229–243 (1987).
21. Nelson, S. J. and Brown, T. R. The accuracy of quantification from 1D NMR spectra using the PIQABLE algorithm. *J. Magn. Reson.* **84**, 95–109 (1989).
22. Bates, T. E., Williams, S. R. and Gadian, D. G. Phosphodiesters in the liver: the effect of field strength on the ^{31}P signal. *Magn. Reson. Med.* **12**, 145–150 (1989).
23. Clarke, D. D., Lajtha, A. L. and Maker, H. S. Basic Neurochemistry. In *Intermediary Metabolism*, ed. by G. J. Siegel, p. 558 (1989).
24. Freeman, D., Sailasuta, N., Tropp, J. and Hurd, R. An efficient CW nuclear Overhauser enhancement of *in vivo* ^{31}P NMR. *10th Annual Meeting of the Society of Magnetic Resonance in Medicine.* Abstr., p. 1019 (1991).
25. Kolem, H., Schneider, M., Wicklow, K. and Sauter, R. Fast *in vivo* phosphorus spectroscopy using nuclear Overhauser enhancement. *9th Annual Meeting of the Society of Magnetic Resonance in Medicine.* Abstr., p. 889 (1990).
26. Bachert-Baumann, P., Ermark, R., Bellemann, M. E., Semmler, W. and Lorenz, W. J. Signal enhancements in ^{31}P-^{1}H magnetic resonance experiments *in vivo* using broadband decoupling or non-selective presaturation at ^{1}H frequency. *9th Annual Meeting of the Society of Magnetic Resonance in Medicine.* Abstr., p. 1070 (1990).
27. Brown, T. R., Stoyanova, R., Srinivasan, R., Willard, T., Kosinski, E. and Murphy-Boesch, J. Proton decoupled T_1's and NOE enhancements of phosphorus metabolites in the calf. *10th Annual Meeting of the Society of Magnetic Resonance in Medicine.* Abstr., p. 550 (1991).
28. Negendank, W., Crowley, M. G., Ryan, J. R., Keller, N. A. and Evelhoch, J. L. Combined ^{1}H MRI and ^{31}P MRS for diagnosis of bone and soft tissue lesions. *Radiology* **173**, 181–188 (1989).
29. Evelhoch, J. L., Keller, N. A. and Corbett, T. H. Response-specific adriamycin sensitivity markers provided

by *in vivo* ^{31}P nuclear magnetic resonance spectroscopy in murine mammary adenocarcinomas. *Cancer Res.* **47**, 3396–3401 (1987).
30. Maris, J. M., Evans, A. E. and McLaughlin, A. C. ^{31}P nuclear magnetic resonance spectroscopic investigation of human neuroblastoma *in situ*. *New Engl. J. Med.* **312**, 1500–1505 (1985).
31. Pelech, S. L. and Vance, D. E. Signal transduction via phosphatidylcholine cycles. *TIBS* **14**, 28–30 (1989).
32. Naruse, S. and Hirakawa, K. Brain edema studied by magnetic resonance. *Sem. Neurol.* **6**, 53–64 (1986).

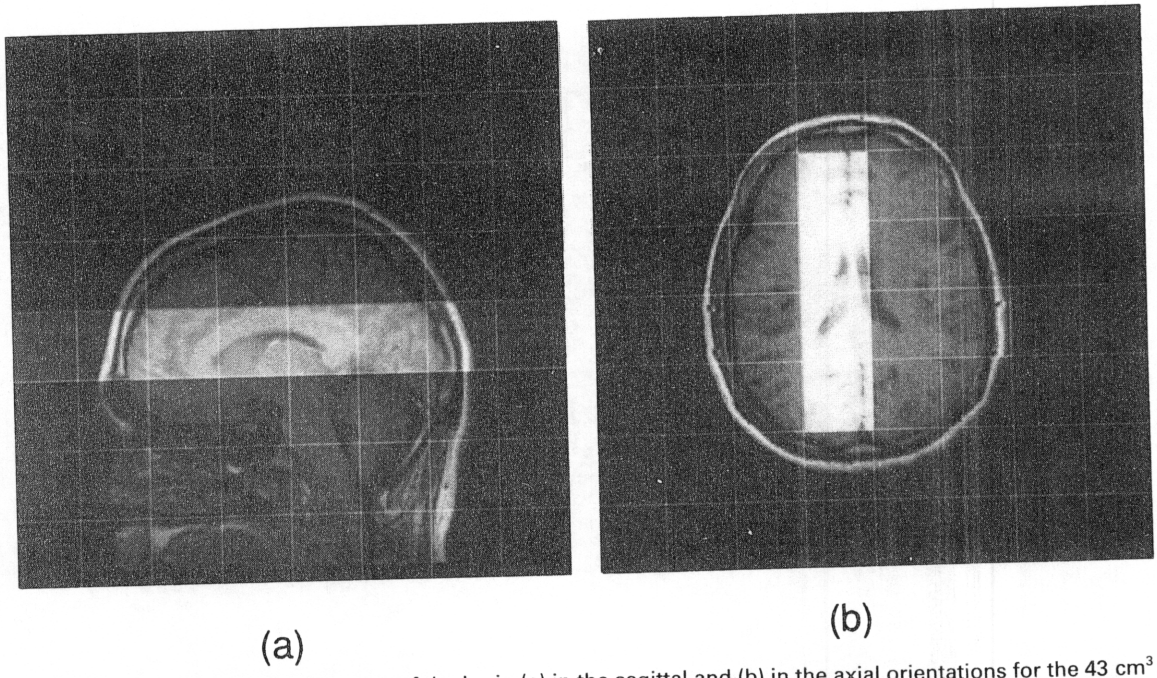

Figure 3. T_1 weighted proton images of the brain (a) in the sagittal and (b) in the axial orientations for the 43 cm^3 (3.5 cm × 3.5 cm × 3.5 cm) examination. The grid indicates the position of the CSI array after voxel shifting of CSI spectra; highlighting indicates the slice and position of the voxels from which the spectra in Fig. 4 were taken.

The areas of various peaks were then determined in the irradiated and non-irradiated cases to estimate the NOE enhancements for this individual, which were ca 60, 25 and 25% for PME, P_i and PCr, respectively. The peak areas of the NTP resonances were the same to within 10%. Even with the addition of the spectra, it was still not possible to evaluate the NOE enhancement in the PDE region because of the presence of a broad peak believed to originate from partially motionally narrowed resonances of phospholipids[22] in the coupled spectrum. The static field homogeneity in the brain could be followed by monitoring the linewidth of the PCr peak. In Fig. 4(b), the third voxel is better shimmed than the others, possibly due to the absence of nearby air–tissue interfaces. The natural linewidth of PCr for this voxel was ca 3 Hz. The PME region of this spectrum shows peaks at the chemical shifts expected for PE and PC (4.32 and 3.79 ppm, respectively). Although this does not constitute absolute proof that these peaks correspond to these compounds, they are well known to exist in the brain[23] and are by far the most likely assignments for these two resonances. The PDE region similarly shows two peaks resolved with chemical shifts appropriate for GPC and GPE (0.49 and 1.03 ppm, respectively).

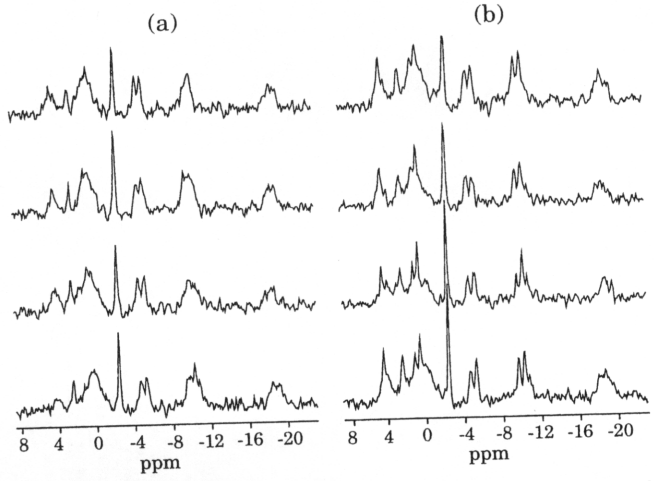

Figure 4. (a) Coupled and (b) decoupled CSI spectra at 43 cm^3 voxel size from the voxels highlighted in Fig. 3 displayed on the same scale. Both CSI data sets were acquired consecutively from the same volunteer with identical acquisition parameters, except for proton irradiation. Filtering in the time-domain for both sets consisted only of a 3 Hz Lorenzian. Baselines estimated for each spectrum have been subtracted.

At higher spatial resolutions the increased resolution and sensitivity from proton irradiation can be used to improve the quality of the metabolic images constructed from the data. To demonstrate this, coupled and decoupled CSI spectra were acquired at 18 cm^3 (2.6 cm × 2.6 cm × 2.6 cm) voxel resolution in consecutive 51 min examinations from a second volunteer. Coupled and decoupled spectra from an axial slice at approximately the same elevation in the brain as the first volunteer are shown in Figs 5(a) and (b), respectively. Metabolite images of the entire PME peak region were constructed from both data sets without spatial filtering or correction for the field profile of the coil and are shown on the same scale in Fig. 6. As one can see, the axial profile of the head is far better defined in the decoupled case than the coupled case, owing to both the improved resolution and signal intensity of the PME metabolites. Some increased signal intensity results from the increased B_1 field around the periphery of the head. Some variations in intensity of the images in the region of the head are related to errors in baseline estimates, and some decrease in intensity of phosphates in the mid-brain region results from the presence of the ventricles. In both the coupled and decoupled data sets, the chemical shift of P_i could be determined more reliably in better shimmed voxels. In the presence of proton irradiation, however, more determinations could be made at this voxel resolution with the improved resolution of the PME and PDE resonances on either side of the P_i resonance. In the present circumstances, no significant variations were

^{1}H-^{31}P multiplet structures and an increase in peak amplitude from NOE enhancement. These two effects arise from quite different interactions and thus are induced by different proton power levels. To achieve decoupling, the power level must be sufficient to average out a J coupling of 10 Hz. This means proton B_1 fields should be strong enough to average out a proton's spin state in <100 ms. The NOE enhancement on the other hand can be achieved by only saturating the proton spins. This requires substantially less power since the typical T_1 is 500 ms. Thus, bi-level power was used: 13 W during acquisition to achieve decoupling and 1.5 W during recovery to maintain proton saturation. Assuming water protons are the dominant relaxation pathway for ^{31}P in tissue,[24] we can estimate the effects of our CW radiation 1 ppm downfield from water.[2] Taking a $T_1 = 500$ ms and a $T_2 = 50$ ms, the water protons are >90% saturated by this radiation. The same computation would yield a saturation of 99% using the magnitude of the decoupling field (200 Hz), although the saturation effect of this irradiation is complicated by the Waltz-4 modulation. Nevertheless, we should thus be observing at least 90% of any possible NOE from water protons. Bi-level irradiation with CW was chosen over other ^{1}H excitation, such non-selective 180° pulses,[25] because of its ease of implementation, the relatively small power it contributes (25% of total), and its independence of the *TR* and the T_1s of the individual metabolites. Although we have not yet studied enough individuals to report population values for the NOE enhancements in brain, the observed differences in NOE enhancements between the individuals we have studied appear to be small. Interestingly, while NTP exhibits almost no NOE enhancement in brain, a significant NOE enhancement is observed in calf muscle.[3,26,27] This tissue difference means that a localized study is needed to determine the NOE enhancements in the brain, since any measurements on the whole head would be contaminated by muscle.

Decoupling of the ^{1}H-^{31}P multiplet structure is particularly useful in the PME and PDE regions. As can be seen from the spectra shown in Figs 2, 4 and 6, substantial improvements in resolution, and thus, metabolite identification, are apparent. The PDE region shows two narrow peaks which correspond in chemical shift to GPE and GPC. These peaks overlap a much broader peak which presumably arises from the head groups of the phospholipids in the cell membranes.[22] The PME region similarly shows two peaks which have chemical shifts appropriate for PE and PC at pH 7. PE and PC are known to exist in brain (PE at a concentration of 1.1 mM),[23] thought to be altered in tumors,[28–30] and may be involved in some of the fundamental processes involving cell division.[31] The ability to distinguish and measure the amounts of these compounds present in brain tumors may provide a unique window to the biochemistry of this important class of brain pathologies. Since animal experiments suggest the relative amounts of PC or PE can be a measure of therapeutic response,[29] the ability to measure the two compounds individually is potentially of great importance. Although our processing software does not now separate the individual resonances of these compounds, future developments which will apply techniques to resolve multicomponent lines to the individual spectra from each voxel will permit us to determine the spatial distributions of each of these compounds individually.

In addition to the increase in resolution in the PME and PDE regions, the reduction of overlap with the P_i peak improves our ability to observe P_i in voxels throughout the brain. Resolving P_i accurately makes it possible to determine both its spatial distribution and, from its chemical shift, the regional pH, a parameter of considerable importance for many brain dysfunctions. It is likely that the P_i concentration is also a parameter of considerable importance since it is so closely coupled to the amount of available metabolic energy through the NTP free energy. In animal model studies, strong

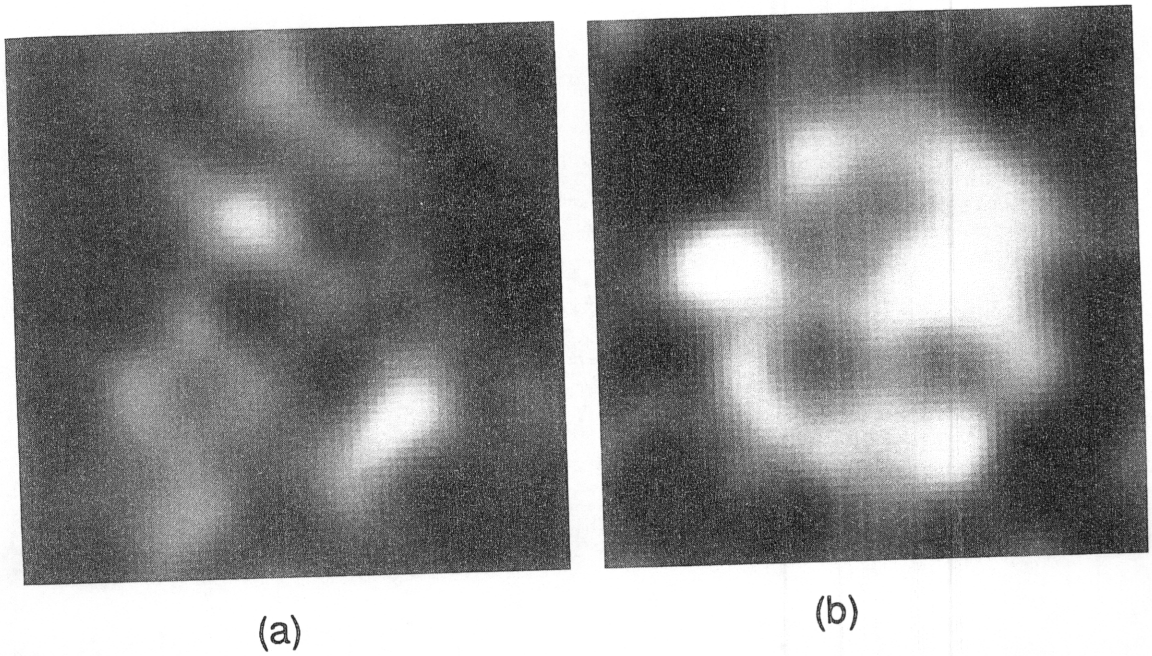

Figure 6. Metabolite images of PME constructed from (a) coupled and (b) the decoupled CSI datasets of Figs 5(a) and (b), respectively. Intensities are scaled to the maximum intensity of the decoupled data.